Effect of carbon fiber oxidization parameters and sizing deposition levels on the fiber-matrix interfacial shear strength

Filip Stojcevski[a,b,*], Timothy B. Hilditch[a], Thomas R. Gengenbach[c], Luke C. Henderson[b,*]

[a] Deakin University, School of Engineering, Pigdons Road, Waurn Ponds Campus, Geelong 3216, Victoria, Australia
[b] Deakin University, Institute for Frontier Materials, Pigdons Road, Waurn Ponds Campus, Geelong 3216, Victoria, Australia
[c] CSIRO Manufacturing, Bayview Avenue, Clayton, VIC 3168, Australia

ARTICLE INFO

ABSTRACT

This paper investigates fifteen fiber types against two epoxy resin systems and the effects of altering electrochemical oxidization conditions and sizing deposition ratio on interfacial shear strength (IFSS). Oxidization current was altered between 0, 2, and 3.4 A while sizing deposition ratio was altered between unsized, 1:10, 1:15 and 1:20 parts sizing to water. Desized fibers were also compared against pristine unsized fibers. Results show, a correlation between increasing current and IFSS, however sizing has an optimal ratio for best performance. Improvements through oxidization are attributed to the introduction of oxygenated functional groups on the fiber surface while improvements due to sizing are attributed to the promotion of a chemically active intermediate layer between the fiber and resin. Fiber roughness was seen to play no effect on IFSS. Desized fibers and unsized fibers had similar IFSS results however characterisation shows chemical composition of the fiber surfaces to be very different.

1. Introduction

With their high strength to weight ratios contributing to reduction of component structural mass, carbon fiber reinforced polymers have already made a notable mark on the engineering industry [1]. While carbon fiber composites are synonymous with high performance materials, micro-cracking, a known failure mechanism of these materials commonly arises as a result of a weak interface between fibers and resin. One means to obviate this limitation is to chemically modify the surface of carbon fibers to promote fiber/resin compatibility, which typically results in a simultaneous increases in fiber/matrix adhesion [2–4]. For this reason surface treatments have become of intense interest, with a number of reviews published on the topic recently [5–7]. Over the past decade many oxidative and non-oxidative techniques have been employed to etch [8–10], roughen [11,12], and alter surface chemistry [10,13,14] with varying degrees of success. Whilst much of this research demonstrates enormous promise, uncertainties still remain in interfacial science.

Academic consensus between the relative contribution of different bonding mechanisms, namely chemical adhesion, mechanical interlocking or fiber wetting, that constitutes an improved interfacial bond remains contested. The influence of several manufacturing variables during carbon fiber fabrication and final interfacial performance is also unclear, as is the relationship among these variables. Likewise performance comparison among sized, desized and pristine virgin fibers remains ambiguous requiring further study.

In this work we have used a pilot scale carbon fiber line (www.carbonnexus.com.au) for the manufacture of virgin carbon fibers to enable the examination of bonding interactions in an industrially relevant manner. The goal is to clarify the effects of two processing parameters; electrolytic bath amperage and sizing deposition ratio, on interfacial shear strength (IFSS). It is generally agreed that the surface treatment is critical to ensure improved IFSS [13–15]. Studies have attributed the importance of the electrochemical oxidization to be the removal of weakly bound graphite from the surface of the fiber and the introduction of polar functional groups (e.g. carboxylic acids, phenols, ketones, etc.) [7,11]. However no systematic study on varying electrochemical amperage and subsequent effects on IFSS has been conducted. Conversely, the influence of sizing compatibility and whether its effects are beneficial [8,16–18] or detrimental [12,13,19] to IFSS performance have not reached a unified scientific consensus. This convolution alone constitutes the requirement for further research but by adding manufacturing variables such as the effects of oxidization, the requirement for this research becomes crucial (see Table 1).

Conflicting literature is also observed within studies claiming mechanical interlocking to improve IFSS [12,19] while others show no

---

Table 1
Fiber classifications table within this study.

	Unsized (S0)	Desized (D)	Sized (S20)	Sized (S15)	Sized (S10)
0 A	0 A-S0	0 A-D	0 A-S20	0 A-S15	0 A-S10
2 A	2 A-S0	2 A-D	2 A-S20	2 A-S15	2 A-S10
3.4 A	3.4 A-S0	3.4 A-D	3.4 A-S20	3.4 A-S15	3.4 A-S10

evidence of this [20]. Similarly contentions supporting polar functional groups [8,10,19,20] and dispersive functional groups respectively [13,18] as the key contributor of improved IFSS highlight gaps in scientific understanding that require further exploration [7,21]. The truth may be more complex and rather than a uniform answer, may be a matter of fiber-resin compatibility to be considered on a case by case basis [22]. In either case further fundamental research is required.

Reasons for these aforementioned discrepancies are likely due to numerous factors. Firstly, the constituents of commercial sizings are typically not publicly known and thus a comparison of two sizings may not be strictly scientific as more than one variable may be changed without control. Secondly the ability to examine both surface treatments and sizings separately and simultaneously to observe any masking or interaction effects has not been afforded to researchers without access to a commercial manufacturing line. This has fostered a third issue, with fibers in the majority of previous studies that first desized and then subsequently resized or surface treated as sizing is routinely applied in the manufacture of commercial fiber [13,15]. Undoubtedly this process introduces further variability in testing control which may not necessarily give an accurate representation of virgin carbon fibers.

In this work, we report our findings focussing on the effects of surface treatment and sizing processes on IFSS. These manufacturing effects are observed individually (i.e. impact of only sizing or only oxidization), and simultaneously (impact of both sizing and oxidization together). Results of treated pristine fibers are also compared against fibers that have been desized and then treated to understand if the desizing process alters the subsequent IFSS. Extensive physical and chemical characterisation was done on all fibers to compile an accurate understanding of fiber properties.

It was concluded that each of these processes (surface treatment and sizing) improved IFSS independently with no masking effects influencing results. Improved IFSS was observed to be a factor of both chemical modification introducing active groups to the surface and sizing dispersion encouraging a greater fiber/matrix compatibility at the interface. Mechanical interlocking (improvement in interfacial adhesion attributed to fiber surface roughness) was not seen to play any statistically significant role on IFSS. Desized fibers were also observed to provide mixed results suggesting that they may not necessarily be representative of pristine fibers.

2. Materials and methods

2.1. Raw materials

2.1.1. Carbon fibers

CFs were manufactured from a polyacrynitrile (PAN) precursor sourced from Jilin Chemical Industrial Company (China). Fiber tension was maintained at approximately 600 cN during fabrication. Stabilisation oven temperature was increased from 230 °C to 260 °C across 4 heating regions, each 20 m in draw length. Across the low temperature (LT) and high temperate (HT) carbonisation furnaces, temperature increased from 650 °C to 850 °C (LT) and 1100 °C to 1450 °C (HT) respectively. Combined LT and HT furnace draw length was 6 m.

Following carbonisation, fibers underwent electrochemical oxidization and sizing treatment. These are the two variables being considered within this investigation. Ammonium bicarbonate with a conductivity of 20.4 mS/cm was used as the treatment electrolyte. The amperage passing though the electrolytic bath was altered among 0 A (unoxidized), 2 A and 3.4 A. After oxidization, fibers were washed using DI-water and dried before entering a sizing bath. Sizing solution was created by dissolving Epoxy 834 (Hexion, USA) into water and thoroughly mixing. The ratio of Epoxy 834 sizing to water was varied among 1:20, 1:15 and 1:10. Unsized fibers were also manufactured. All fibers underwent a final drying process before being spooled and packaged.

It is especially with noting that due to the strict control of electrolytic conductivity, amperage and voltage are not able to be decoupled during electrochemical oxidization. Thereby an increase in amperage also increases voltage. Under the 2 A condition a 12.6 V potential was applied while the 3.4 A condition used 18.0 V potential. While for the remained of this report fiber conditions will be referred to by their "amperage condition" the reader is encourage to keep in mind the relationship that exists between voltage and current.

By altering the electrochemical oxidization bath amperage and sizing the following 12 fibers were manufactured. Codes 0 A, 2 A and 3.4 A denote oxidative treatment (0 A, 2 A and 3.4 A, *respectively*), and S0, S20, S15, S10 denote sizing ratios (Unsized, 1:20 thinly sized, 1:15 moderate sized, 1:10 heavily sized, *respectively*).

Three fibers were also desized to compare performance against pristine fibers. A small batch of pristine fibers with a 1:15 sizing ratio was cut and subjected to soxhlet extraction in acetone at 70 °C for 20 h. They were then air dried ready for testing. Code letter D denotes the desized fibers.

2.1.2. Resins

Two epoxy resins were used in testing. *Resin one* was RIMR 935 mixed with RIMH 937 hardener at a 1:04 parts by weight ratio (Hexion, America). *Resin two* was a mixture of Bisphenol A diglycidyl ether (DGEBA) mixed with 4,4′-Diaminodiphenylmethane (DDM) at a weight ratio of 1:0.3 (Sigma-Aldrich, Germany). Both resins were cured at room temperature for 48 h, then post cured at 100 °C for 12 h. Each matrix will be referred to as *resin one* or *resin two* for the remainder of this paper for simplicity, unless resin chemistry is specifically considered. FT-IR spectra of each resin is available in the electronic Supplementary Information (ESI).

Supplementary data associated with this article can be found, in the online version, at https://doi.org/10.1016/j.compositesa.2018.08.022.

2.2. Testing

2.2.1. Tensile strength of single CF

Fiber tensile strength and modulus was determined using a Favimat single fiber tester (Textechno H. Stein, Germany). Single fibers at a length of 5 mm were loaded between two clamps with a 0.8 g pre-weight attached. The Favimat robot then tensions the fibers to failure. Elongation, linear density, Youngs modulus and tensile strength at failure were recorded. 60 samples of each fiber type were tested.

A Weibull probability (P) distribution was performed for all fiber configurations. This two-parameter probability analysis provides the cumulative probability of each carbon fiber configuration to undergo premature failure. A linear distribution of data points denotes confidence in fiber variability being negligible within mechanical testing.

$$P = 1 - \exp\left[-\left(\frac{\sigma}{\sigma_0} \right)^m \right]$$

(1.1)

σ is the applied tensile strength, m is the Weibull shape parameter/modulus and σ_0 is the characteristic fiber stress. For each fiber configuration the tensile strength results were arranged from smallest to largest and P for each data point was determined using the median rank method:

$$P = \frac{i-0.3}{n + 0.4} \quad (1.2)$$

where n is the total number of samples run (n = 60) for the given configuration and i is the tenacity ordered rank.

Using a linear regression of the data points the Weibull shape parameter and characteristic stresses are determined. These are required in determining the IFSS for SFFT (Section 2.2.2).

2.2.2. Single fiber fragmentation testing (SFFT)

To manufacture SFFT test specimens, single fibers were isolated from pristine tow bundles and cut to a 45 cm length. At either end of the single fiber, sticky tape was folded and a wooden peg attached to the fibers. Using the pegs, fibers were then movable and placed in a specially designed silicon mould and pre-tensioned at 3.4 mN by the weight of the pegs on either side. Resin was then carefully ejected into the silicon mould using a 3 mL syringe and allowed to cure (refer to Section 2.1). Following post cure, samples were demoulded and polished to remove any imperfections (Fig. 1).

Samples were then loaded into a 50 kN Instron machine where mechanical jaw clamps were tightened to the dog-bone ends allowing an effective elongation length of 25 mm. Bluehill-3 software was used to create a loading program in accordance with SFFT testing protocol [23]. An elongation loading rate of 0.05 mm/min was used. Each sample was loaded for 50 min.

SFFT works by using the differences in elongation properties between the resin and carbon fibers. As the micro-composite samples are loaded, stress at the interface between the fiber and resin increases. Stresses at the interface ultimately reach a level that exceeds the tensile strength of fibers and the fiber fragments. As loading continues fiber fragmentation is repeated until the stress transfer at the interface can no longer reach the fiber fracture strength required. This point is known as fragment saturation. Dependent on the quality of the interfacial bond the average fragment lengths at saturation will vary. A strong interface requires less area to facilitate a greater level of stress transfer causing smaller but more numerous fragments. For further information of fragment patterns and SFFT interested readers can refer to references [24–26].

Subsequent to Instron loading, samples were examined under a polarised optical microscope to measure fragment length. An Olympus DP70 Optical Microscope was used to measure fragment length and the critical fragment crack length (l_c) calculated using Eq. (2.1).

$$l_c = \frac{4}{3} \bar{l} \quad (2.1)$$

By calculating the critical crack length, l_c, and introducing the tensile strength values obtained in Section 2.2.1, IFSS was calculated (Eq. (2.2). For each fiber/resin configuration 5 micro-composite samples were tested.
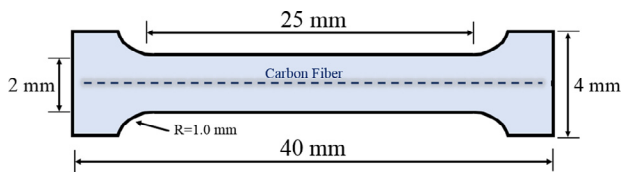
$$\tau = \frac{\sigma_f d}{2l_c} \quad (2.2)$$

Fig. 1. Single fiber fragment testing dog-bone specimen. (For interpretation of the references to colour in this figure legend, the reader is referred to the web version of this article.)

2.3. Characterisation

2.3.1. Atomic force microscopy (AFM) analysis

Surface roughness of fibers was determined using contact mode atomic force microscopy (AFM). A Bruker Dimension SPM 3000 microscope was used at a 0.5 μm/min scan rate. A cantilever tip with a spring constant of 0.12 N/m and silicon nitride pyramid probe was used. 3 individual fibers per fiber variant were mounted on glass slides. 27 images were taken on a $1 \times 1\,\mu$m scale and 9 images on a $3 \times 3\mu$m scale for each fiber type.

Images were imported to NanoScope Analysis 1.4 software and a second order flattening applied to remove any fiber curvature. Arithmetic roughness average (Ra) was thereby calculated using Eq. (3.1).

$$R_a = \frac{1}{L} \int_0^L |Z(x)| \, dx \quad (3.1)$$

where Z(x) is the depth of peaks and troughs on the fiber surface and L is the length of scan.

2.3.2. Contact angle and surface free energy

Wettability refers to the ability of a solid material to create a common interface with a liquid. This characteristic is governed by surface free energies of both the liquid and solid surface. As the polar and dispersive surface energy components of liquids are known, fibers can be suspended into various liquids and data extrapolated from the subsequent meniscus angle formed. Further in-depth analysis of the contact energy methods can be found in references [12,27,28].

Youngs equation (Eq. (4.1) establishes the phenomenon of thermodynamic wetting that describes the impact of a contact angle being created between a fiber and resin [19,20].

$$\gamma_{SV} = \gamma_{SL} + \gamma_{LV} \cos(\theta) \quad (4.1)$$

where γ_{SL} is the surface tension at the solid-liquid interface, γ_{LV} the liquid-gas interface, γ_{SV} the solid gas interface and θ is the equilibrium contact angle. From this foundation several methods of subcategorising surface energy into dispersive (D) and polar (P) energy are available. Within this study the Owens-Wendt-Rabel-Kaelble (OWRK) method was used as it separates energy into these two parameters alone [12].

$$\gamma_L = \gamma_L^P + \gamma_L^D \quad (4.2)$$

$$\gamma_S = \gamma_S^P + \gamma_S^D \quad (4.3)$$

Through mathematical derivation the Owens-Wendt equations can be rearranged into the following:

$$\gamma_{SL} = \gamma_{SV} + \gamma_{LV} - 2\sqrt{\gamma_{SV}^D \gamma_{LV}^D} - 2\sqrt{\gamma_{SV}^P \gamma_{LV}^P} \quad (4.4)$$

Eq. (4.5) presents a rearrangement that follows a linear equation format ($y = mx + c$) which is extrapolated by plotting contact angle data points. The squared values of both the vertical axis intercept and gradient in the linear equation are dispersive and polar surface energy of the solid material being testing; namely fibers.

$$\frac{(1 + \cos\theta)\gamma_L}{2\sqrt{\gamma_L^D}} = \sqrt{\gamma_s^P}\sqrt{\frac{\gamma_L^P}{\gamma_L^D}} + \sqrt{\gamma_S^D} \quad (4.5)$$

Contact angle testing was conducted by dipping the carbon fiber tows into four different solvents with varying polar and dispersive properties. The subsequent meniscus created by this fiber/solvent interaction was recorded and surface energy calculated using Eq. (4.5). The solvents used were deionised water ($\gamma_L = 72.8$ mN/m, $\gamma_L^D = 22$ mN/m, $\gamma_L^P = 50.7$ mN/m), heptane ($\gamma_L = 20.1$ mN/m, $\gamma_L^D = 20.1$ mN/m, $\gamma_L^P = 0$ mN/m), glycerol ($\gamma_L = 63.4$ mN/m, $\gamma_L^D = 37$ mN/m, $\gamma_L^P = 26.4$ mN/m) and methanol ($\gamma_L = 22.5$ mN/m, $\gamma_L^D = 18.2$ mN/m, $\gamma_L^P = 2.6$ mN/m).

An Attension Contact Angle instrument with a high resolution digital camera was used for measurement. Attension Theta software recorded meniscus formation and contact angle.

2.3.3. X-ray photon spectroscopy (XPS)

XPS analysis was performed using an AXIS Ultra-DLD spectrometer (Kratos Analytical Inc., Manchester, UK) with a monochromated Al K$_\alpha$ source (hν = 1486.6 eV) at a power of 150 W (15 kV × 10 mA), a hemispherical analyser operating in the fixed analyser transmission mode and the standard aperture (analysis area: 0.3 mm × 0.7 mm). The total pressure in the main vacuum chamber during analysis was typically below 10^{-8} mbar.

Bundles of fibres were suspended across a custom-designed frame attached to standard sample bars. This ensured that only the sample to be analysed was exposed to the X-ray beam and that any signal other than that originating from carbon fibres was excluded. Each specimen was analysed at a photoelectron emission angle of 0° as measured from the surface normal (corresponding to a take-off angle of 90° as measured from the sample surface). However, since the microscopic emission angle is ill-defined for fibres the XPS analysis depth may vary between 0 nm and approx. 10 nm (maximum sampling depth). Data processing was performed using CasaXPS processing software version 2.3.15 (Casa Software Ltd., Teignmouth, UK). All elements present were identified from survey spectra (acquired at a pass energy of 160 eV). To obtain more detailed information about chemical structure, C 1s, O 1s and N 1s high resolution spectra were recorded at 40 eV pass energy (yielding a typical peak width for polymers of 1.0 eV). If required these data were quantified using a Simplex algorithm in order to calculate optimized curve-fits and thus to determine the contributions from specific functional groups. The atomic concentrations of the detected elements were calculated using integral peak intensities and the sensitivity factors supplied by the manufacturer. Atomic concentrations are given relative to the total concentration of carbon as follows: the concentration of a given element X was divided by the total concentration of carbon and is presented here as the atom number ratio (or atomic ratio) X/C. This value is more robust than concentrations when comparing different samples. Binding energies were referenced to the aliphatic hydrocarbon peak at 285.0 eV. The accuracy associated with quantitative XPS is ca. 10–15%. Precision (i.e. reproducibility) depends on the signal/noise ratio but is usually much better than 5%. The latter is relevant when comparing similar samples.

3. Results and discussion

3.1. Physical characterisation of fibers

Table 2 provides the tensile strength of the fibers examined within this study. Few statistically significant changes were observed across each sizing fiber set, suggesting that the surface treatment bath did not irreversibly damage the fibers through the introduction of fiber surface defects. Minor discrepancies may be explained by the unavoidable variations in control and environmental parameters observed during manufacturing. However of all fiber sets the S10 fibers had the lowest tensile strength. It must be noted authors of this study are **not** attributing this drop to manufacturing. Rather the tensile strength reduction is theorised to be an introduced flaw during single fiber extraction from pristine tow bundles. In testing of single fibers mechanical properties

(Section 2.2.1), fibers were extracted from tow bundles. The authors observe that the S10 sized fibers create an extremely sticky and difficult to separate tow bundle. This issue was not as prevalent in any other condition which fray easily when not under tension. Whilst challenging to extract fibers, it was still possible, however, the effort required was highly likely to introduce defects.

Table 3 provides the Youngs modulus of fibers being investigated in this study. Variation amongst all fibers excluding the S10 sized fibers were found to be within statistical error margins. S10 sized fibers showed an average modulus reduction of 10–15 GPa however with consideration of error margins, these reduction are not excessive but are noted for research transparency. Cause of modulus reduction are **not** attributed to the use of sizing but rather an influence of tensioning and environmental variation across the LT and HT furnaces. Fibers showing statistically different results are marked in Table 3 accordingly. All fibers listed are still being considered applicable for this study in examining the effects of sizing and oxidization impact.

Additional characterisation data such as **elongation at break, linear density, and failure stress** are provided in the electronic Supplementary Information (ESI).

3.2. Interfacial shear strength

3.2.1. Amperage effects

Complimentary data relating to Fig. 2 are found in Table 4. Fig. 2 shows IFSS results of fibers embedded in resin one. Results are grouped according to oxidization bath amperage. Blue represents 0 A treated fibers, black represents 2 A treated fibers and red represent 3.4 A treated fibers. This colour grouping is also used in Fig. 3.

By categorising IFSS results into common amperages, the effects of varying sizing deposition level (S0, S20, S15 and S10) is observable. Results in Fig. 2 show that across all three categories unsized fibers (S0) performed poorest with respect to their sized counterparts suggesting that sizing is beneficial to interfacial adhesion. Conversely the best performing fibers in all cases were those sized with moderate sizing (S15). The difference between unsized fibers and the S15 sized fibers was 11.4 MPa, 12.7 MPa and 12.5 MPa respectively for 0 A, 2 A and 3.4 A. These correspond to increases of 56.1%, 44.3% and 38.4% respectively between unsized and S15 sized fibers.

This trend creates a parabolic curve that suggests sizing to have an optimal point for improved adhesion. Fibers that used excessive thick (S10) or thin (S20) sizing ratios were found to have IFSS significantly less than the S15 optimised point and not within error margins. However in these cases, average IFSS performance was still improved on unsized fibers. These results concluded two things. Firstly an epoxy sizing in an epoxy matrix was found to improve IFSS. This observation fits conclusions drawn by previous researchers that concluded epoxy sizings is a means to improve IFSS in epoxy resins [29,14,30]. Secondly the sizing to water ratio for water emulsified sizings can be optimised to improve IFSS for all three different amperage groups.

Fig. 3, with corresponding data available in Table 5, shows the effects of fibers in resin two. IFSS results using this resin were similar to those for resin one (see Fig. 2), however IFSS magnitudes were less pronounced across the three sized fiber categories. Unsized fibers again provided the lowest IFSS results under each amperage category with the only outlier being at 0 A where the unsized and S10 fibers performed near identically. Conversely S15 treated fibers provided the highest

Table 2
Tensile strength (MPa) of fibers manufactured in this study.

Current	Unsized (S0)	Desized (D)	Sizing (S20)	Sizing (S15)	Sizing (S10)
0 A	3.59 ± 0.84	3.91 ± 0.75	3.92 ± 0.73	3.42 ± 0.77	3.20 ± 0.65
2 A	3.70 ± 0.60	3.58 ± 0.70	3.73 ± 0.77	3.67 ± 0.89	3.32 ± 0.66
3.4 A	4.10 ± 0.72	3.97 ± 0.60	3.85 ± 0.66	3.54 ± 0.86	3.34 ± 0.66

Table 3
Youngs Modulus (GPa) of fibers manufactured in this study.

Current	Unsized (S0)	Desized (D)	Sizing (S20)	Sizing (S15)	Sizing (S10)
0 A	256.2 ± 14.9	256.7 ± 5.9	257.7 ± 6.3	251.6 ± 5.9	240.1 ± 16.4
2 A	259.2 ± 6.0	257.8 ± 5.2	257.6 ± 6.2	252.7 ± 11.2	232.9 ± 11.4
3.4 A	263.7 ± 7.3	256.6 ± 5.0	252.8 ± 11.5	251.8 ± 9.6	238.9 ± 13.1

IFSS in all cases. Variance between S20, S15 and S10 was within statistical difference in the 2 A and 3.4 A conditions however trends still notable. The difference between unsized (S0) and S15 fibers across the 0 A, 2 A and 3.4 A categories respectively was 14.9 MPa, 11.9 MPa and 17.4 MPa. These correspond to increases of 55.2%, 44.9% and 53.8% respectively, which correspond strongly to the outcomes observed for resin one.

The trends of Fig. 3 leads to similar conclusions drawn from Fig. 2. In that sizing improves IFSS and that there is an idealised ratio that may be optimised to enhance IFSS performance. This idealised ratio was not as pronounced using resin two suggesting resin chemistry does play a role on IFSS and subsequent compatibility to sizing. The use of a sizing that leads to low sensitivity with respect to ratios and IFSS can generally be considered advantageous to manufacturing from a process cost and robustness perspective.

3.2.2. Sizing effects

Fig. 4, with complimentary data in Table 6, shows the IFSS results of fibers embedded in resin one organised and grouped by sizing content. Results are colour coordinated according to the sizing condition. Blue represents unsized (S0) fibers, black represents S20 fibers, red represents S15 fibers and green represents S10 fibers. This colour classification is also applied to Fig. 5.

The results in Fig. 4 show matching trends in that fibers that did not undergo any electrochemical oxidization (0 A) result in the lowest IFSS, and a direct positive correlation between increased amperage during oxidization and IFSS exists. Increases in IFSS from 0 A to 2 A conditions were 8.3 MPa, 5.4 MPa, 9.6 MPa and 9.9 MPa for the unsized, S20, S15 and S10 sizing categories respectively. These values correspond to a 40.9%, 20.8%, 30.2% and 35.4% increase in IFSS respectively across said categories. Comparatively increases from the 0 A to 3.4 A condition were 12.2 MPa, 6.8 MPa, 13.3 MPa and 9.8 MPa for the unsized, S20, S15 and S10 sizing categories. This equate to increases of 59.7%, 26.3%, 41.7% and 35.1% accordingly.

Increasing amperage during oxidization increases IFSS from between 26.3% to up to 59.7% for 3.4 A and 20.8% to 40.8% for 2 A. Improved performance was observed across all four sizing levels suggesting that sizing does not mask the improvements introduced by the oxidization process. Unsized fibers were seen to have the highest relative percentage increases in IFSS. Overall the results in Fig. 4 demonstrate increased amperage during electrochemical oxidization can indeed improve IFSS.

Fig. 5 (corresponding data in Table 7) shows the effects of increased amperage with respect to sizing groups for resin two. Similar trends were observed to those in Fig. 4, however increases were less prominent. For all four sizing groups, IFSS was increased with greater current. For the unsized sizing group, negligible increase occurred from 0 A to 2 A however a 5.3 MPa (19.7%) increase occurred when treated with 3.4 A. Under the S20 condition both 2 A and 3.4 A treatments increased IFSS by 3.6 MPa (10.9%) and 7.6 MPa (22.9%) respectively. The differences between 2 A and 3.4 A treatments were within standard deviation margins. For both the S15 and S10 sized fibers, average IFSS increased with amplified oxidization current. For S15 fibers these increases correspond to 7.6 MPa (22.1%) and 10.0 MPa (29.2%) for 2 A and 3.4 A respectively and for S10 these increases equated to 11.5 MPa (41.6%) and 15.3 MPa (55.6%) respectively. Results suggest that for both resins, using an increased oxidization amperage will improve interfacial adhesion of fibers.

3.2.3. Concurrent effects

From Sections 3.2.1 to 3.2.2 it has been observed that both increased amperage and optimal application of sizing can both improve IFSS. Results showed two distinct trends that do not seem to interfere with one another. Namely the application of sizing did not seem to mask improvements induced by increased oxidization amperage, and the effects of sizing deposition were consistent across all oxidization currents.

However reasonable thought process formulates a question regarding interdependency. Do both these treatments work independently to improve IFSS using different mechanisms, or are they
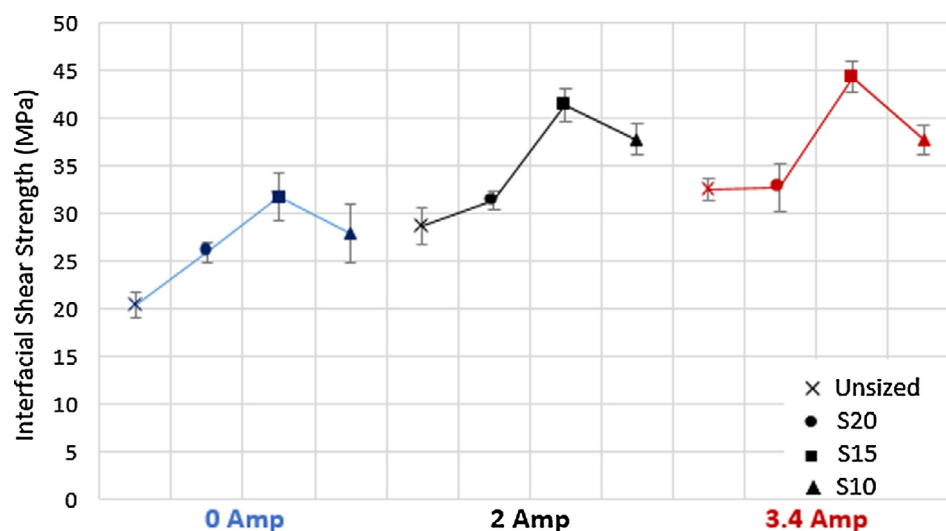

Fig. 2. Effects of sizing on IFSS for fibers embedded in resin one. (For interpretation of the references to colour in this figure legend, the reader is referred to the web version of this article.)

Table 4
IFSS values with standard deviations for fibers in resin one (Fig. 2).

	0 A				2 A				3.4 A			
	Unsized	S20	S15	S10	Unsized	S20	S15	S10	Unsized	S20	S15	S10
IFSS	20.37	25.96	31.80	27.95	28.70	31.37	41.41	37.84	32.54	32.78	45.05	37.75
SD.	1.4	1.0	2.5	3.1	2.0	1.0	1.8	1.6	1.1	2.5	1.6	1.4

working concurrently together? This paper is in a unique position to explore this question as two variables were isolated during fabrication thereby eliminating external noise and allowing a multi-variant analysis to be conducted.

A simple way to assess interdependency is to isolate IFSS improvements attributed specifically to sizing treatments and electrochemical oxidization amperage separately. If the increases observed work independently from one another then IFSS for fibers that undergo both treatments should be predictable by combining results of each independent treatment (Eq. (5). If improvements work concurrently together then predictions will be underestimated suggesting a crossover of mechanisms. Table 8 provides the increases in IFSS attributed to each treatment respectively as observed in testing of resins one and two. (Raw data refer to Sections 3.2.1 and 3.2.2).

By combining the increases of sizing and oxidization amperage in Table 8 together, the IFSS of remaining fibers that underwent both treatments can be predicted (Eq. (5). Table 9 shows the predicted IFSS results and the and experimentally determined IFSS of fibers that had undergone both treatments. The deviation of predicted versus real results is also presented.

$$Predicted = Control + \Delta_{SIZING} + \Delta_{Amps.} \tag{5}$$

Deviation calculations show a mixture of results. When considering resin one, the margin between predicted results and reality was below 10% for all fibers excluding TH-S20, with half of all predictions within 4% accuracy. Comparatively, in resin two, the deviation in prediction increased to be between 10% and 27% for all but one of the fiber cases. Hence the ability to predict IFSS due to treatment conditions is less accurate in resin two. This was somewhat expected as Figs. 3 and 5 in Sections 3.2.1 and 3.2.2 showed less pronounced difference between IFSS values than their respective resin one counterparts. It is also noteworthy that in each case for resin two the measured IFSS was noticeably higher than the predicted value. For resin one the measured value were a mixture of slightly higher or lower.

From these Table 9 predictions authors conclude the following. Sizing and electrochemical treatment are working independently from one another to improve IFSS as suggested by the high accuracy of predictions of resin one. The mechanisms by which they are doing so are further explored later in this paper. However dependant on resin selection these mechanisms may show varied levels of overlap and convolution as suggested by the discrepancy between resin one and two predictions. Importantly two mechanisms seem to be active in improving IFSS.

3.2.4. Desizing effect

Fig. 6 (complimentary data in Table 10) shows the comparison of IFSS results of pristine unsized fibers (S0-T0, S0-TM, S0-TH) and desized fibers subject to three oxidization amperages. SFFT was conducted with fibers embedded in resin one (blue) and resin two (red).

For fibers embedded in resin one, IFSS was near identical for all three oxidization amperages with deviations falling within standard deviation margins. This suggests that fiber that have been desized through soxhlet extraction can provide IFSS representative of pristine fibers. Average deviation across pristine and desized fibers in resin one was below 7.0%.

For fibers embedded in resin two a mixture of results was observed. Fibers that had undergone electrochemical oxidization at 2 A were found to have near identical IFSS values with only a 0.9% margin of difference. Under this oxidization, pristine and desized fibers were considered matching. However for unoxidized fibers (0 A) and 3.4 A oxidized fibers IFSS was statistically different. Pristine unoxidized fibers had on average a 4.7 MPa larger IFSS, and 3.4 A oxidized fibers a 5.4 MPa increase. Under both these conditions pristine fibers performed better. This inconsistency between IFSS values in the two resins may suggest that resin compatibility may play a considerable role when considering if desized and pristine unsized fibers may be considered representative. However, as resin one showed they may provide an effective means to further our understanding of materials science
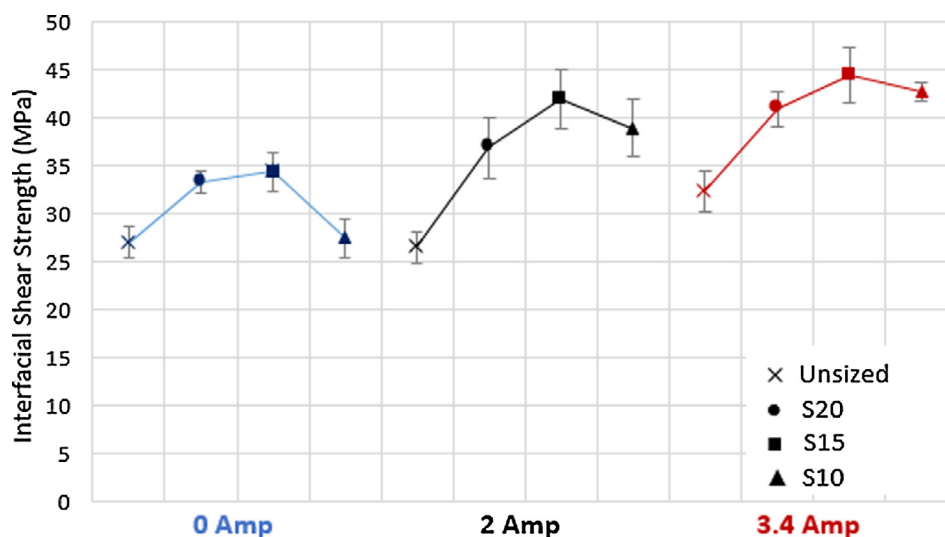

Fig. 3. Effects of sizing on IFSS for fibers embedded in resin two. (For interpretation of the references to colour in this figure legend, the reader is referred to the web version of this article.)

Table 5
IFSS values with standard deviations for fibers in resin two (Fig. 3).

	0 A				2 A				3.4 A			
	Unsized	S20	S15	S10	Unsized	S20	S15	S10	Unsized	S20	S15	S10
IFSS	27.06	33.31	34.39	27.53	26.50	36.96	41.98	38.98	32.40	40.96	44.43	42.83
SD.	1.6	1.2	2.1	2.0	1.7	3.2	3.2	2.9	2.1	1.8	2.9	1.0

especially for researchers limited by access to pristine fibers.

3.3. Characterisation

3.3.1. Roughness effects

The roughness of the fibers in this study were determined using AFM (see Section 2.3.1). Ra values of pristine fibers are presented in Fig. 7 with corresponding data in Table 11. Fibers were grouped according to sizing arrangements. Unsized fibers were observed to have the largest Ra roughness and standard deviation amongst results. Unsized fibers also showed no clear trend of increasing or decreasing roughness with increased oxidization amperage. Coupled with the large error bars, it could not be sufficiently concluded that increased oxidization amperage altered the surface roughness to a notable degree for unsized fibers. This result is contrary to some studies that have observed oxidization treatment to exfoliate the outermost fiber surface to smoothen roughness [18,19].

Conversely S20, S15 and S10 sized fiber conditions were found decrease Ra between 7.2 nm and 12.8 nm, equating to 22% and 40% reductions respectively, compared to the smoothest of unsized fibers (S0-3.4 A). Thus sizing significantly smooth the fiber surface. Across all three sizing groups average roughness was decreased as the oxidization amperage increased. Although error margins showed some overlap, there was a clear trend of average decreasing roughness. Across the S20, S15 and S10 fibers average roughness decrease between untreated 0 A and 3.4 A fibers was 4.3 nm (17.7%), 4.4 nm (17.2%) and 3.6 nm (15.5%) respectively. Hence sizing was found to smoothen the fiber surface and as oxidization increased surface Ra decreased marginally for sized fibers.

Fig. 8 above (complimentary data in Table 11) shows the comparison of Ra roughness's between pristine unsized fibers and desized fibers. Two outcomes were observable. Firstly through desizing, average surface roughness of fibers was decreased by between 9.2 nm and 11.3 nm when compared to the smoothest unsized fiber. Thus desizing undoubtedly smoothened fibers however the means by which this is done is somewhat unclear. By comparing surface roughness of desized fibers to those of the sized fibers, negligible roughness variation is observed. It is theorised that desizing has removed the sizing on the fiber surface (*as supported by XPS data in* Section 3.3.2) however with this process, so has the thin outer layer of carbon that has bonded to the sizing. Consequently the remaining surface was smoothened.

The second outcome is that desized fibers did not show any notable trend related to oxidization amperage. Interestingly desized roughness values fall within average roughness for all sized fiber groups between 21.4 nm and 23.5 nm. However no trend of smoothening with increased oxidization amperage such as those for sized fibers was observed. Hence desized fibers would appear to be less sensitive to oxidization effects however exhibit the same roughness values as sized fibers.

3.3.2. Chemical characterisation of fibers

With the physical properties of these fibers characterised, attention turned to examining the surface chemistry via X-ray photoelectron spectroscopy (XPS). This technique is extremely surface sensitive, with typical sample depths being around 10 nm, and can provide information on the elemental composition and oxidation state of the fiber surface. While XPS studies of oxidised fibers have been conducted previously [8,10] these typically use desized carbon fibers, which is not necessarily typical of an unsized carbon fiber. It is important to note that XPS of carbon fiber surfaces is typically challenging. Because of the heterogeneity of the fiber surface and the complex surface chemical structure it is difficult to reliably and consistently identify, let alone quantify, specific functional groups. The two main spectra of interest in this respect are the C 1s and O 1s photoelectron peaks, however, interpretation of both is problematic because of complicating factors: in the case of the C 1s the intrinsic spectrum of the underlying carbon fiber has the typically complex asymmetric shape of graphitic structures, with a range of additional overlapping peaks superimposed due to different carbon-oxygen functional groups. The O 1s does not experience the same range of chemical shifts as the C 1s and, as a consequence, displays a broad featureless spectral envelope. The prominent
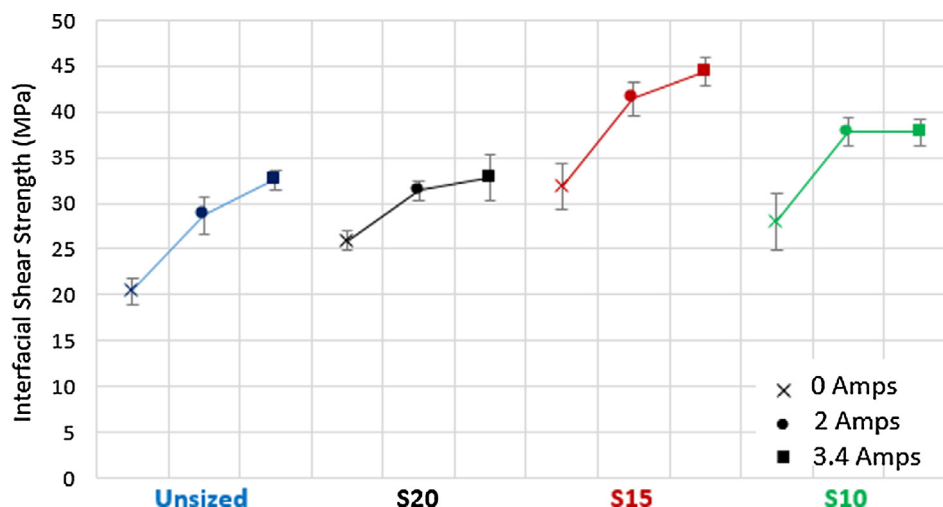

Fig. 4. Effect of amperage on IFSS in resin one. (For interpretation of the references to colour in this figure legend, the reader is referred to the web version of this article.)

Table 6
IFSS values with standard deviations for fibers in resin one (Fig. 4).

	Unsized			S20			S15			S10		
	0 A	2 A	3.4 A	0 A	2 A	3.4 A	0 A	2 A	3.4 A	0 A	2 A	3.4 A
IFSS	20.37	28.70	32.54	25.96	31.37	32.78	31.80	41.41	44.35	27.95	37.84	37.75
SD.	1.4	1.9	1.1	1.0	1.0	2.5	2.5	1.8	1.6	3.1	1.6	1.5

C 1s peak at 286–287 eV binding energy (BE) due to epoxy groups (C-O) represents an exception in the case of sized and partially desized fibres. The relative peak intensity of this peak compared to the main peak at 284.5–285 eV (aliphatic/aromatic hydrocarbon) provides a simple qualitative measure of the relative amount of sizing on the carbon fibre surface. We therefore refrain from employing more advanced data processing techniques such as curve-fitting, since it would neither be quantitative not reliable.

The C 1s spectrum of the unsized and untreated fiber (Fig. 9, left, blue) displays the above-mentioned typical peak shape of graphitic carbon with possibly some intensity at higher BE due to various carbon-oxygen functional groups, as mentioned above, consistent with other examples [8,16,18,31]. Interestingly, after sizing these fibers then subjecting them to soxhlet extraction in acetone for 24 h, a residual shoulder in the XPS spectrum can be observed at 286.5 eV (Fig. 9, red), most likely due to residual sizing. This is confirmed when comparing the C1s spectrum for the epoxy-sized fibers (Fig. 9, greens), which displays a very prominent epoxy signal at the same binding energy.

Further supporting this observation, the O 1s spectrum (Fig. 9, right) for these same fibers shows a broad peak for the unsized and untreated fibers, suggesting an array of chemistries on the fiber surface (Right, blue). After sizing then desizing these fibers the O 1s narrows and moves to approx. 533 eV, a BE, consistent with the increased epoxide oxygen species on the fiber (Right, red). Again, this can be confirmed by a comparison with the corresponding spectrum of sized fibers; thus it is assumed that a trace of the original sizing agent remains on the surface of the desized fibers.

Given the unusual result of residual sizing being present on the surface of the desized untreated fibers, we were curious if this was consistent for oxidised fibers and if the residual amount of sizing was similar. The C1s spectrum of unsized fibers, with increasing applied amperage (Fig. 10, left, blue) shows a similar peak shape as the untreated samples, though with the evolution of a shoulder peak at 288–289 eV. This is consistent with other studies, and this peak is diagnostic of highly oxidised carbon species, typically carboxylic acids.

This makes sense as the higher amperage, corresponds to a higher oxidation potential. Sizing these fibers at a 1:15 ratio followed by the same desizing protocol (soxhlet in refluxing acetone for 24 h) gave an unexpected trend. The amount of residual sizing agent retained on the surface after desizing, increased concurrently with increasing fiber oxidation. This suggests that the higher the polarity of the fiber surface, the more difficult it is to remove the sizing agent via standard desizing techniques. It is possible that the increased polarity of the fiber surface, due to the introduction of carboxylic acids and other carbon-oxygen functional groups, facilitates a large degree of hydrogen bonding to the sizing agent, thus strengthening the adhesion between fiber and sizing agent.

Overall, investigation by XPS of these fibers proved that increasing the oxidation potential results in higher polarity of the fiber surface, and consequently, stronger adhesion between fibre and sizing agent (Table 12). The typical desizing protocol used throughout the literature has been shown to be inadequate in completely removing all sizing agent from the surface of these oxidised and subsequently sized fibers [8,18].

Note that N 1s spectra, elemental compositions (normalised to carbon), and other comparisons between samples are provided in the ESI.

3.3.3. Fiber surface energy

Wettability refers to the ability of a solid material to create a common interface with a liquid. Surface energy may provide an indication of material compatibility however for more in depth discussion on the importance of polar and dispersive surface energy refer to Section 2.3.2.

Table 13 above presents the polar and dispersive energies of all fibers within this study. The polar surface energy did not vary notably with respect to treatments suggesting oxidization and sizing had negligible effect on fiber polarity. Conversely sizing was shown to increase dispersive surface energy as compared to unsized fibers from anywhere between 8.3% (3.4 A, S20) to 54.5% (T0, S20). For these sized fibers an
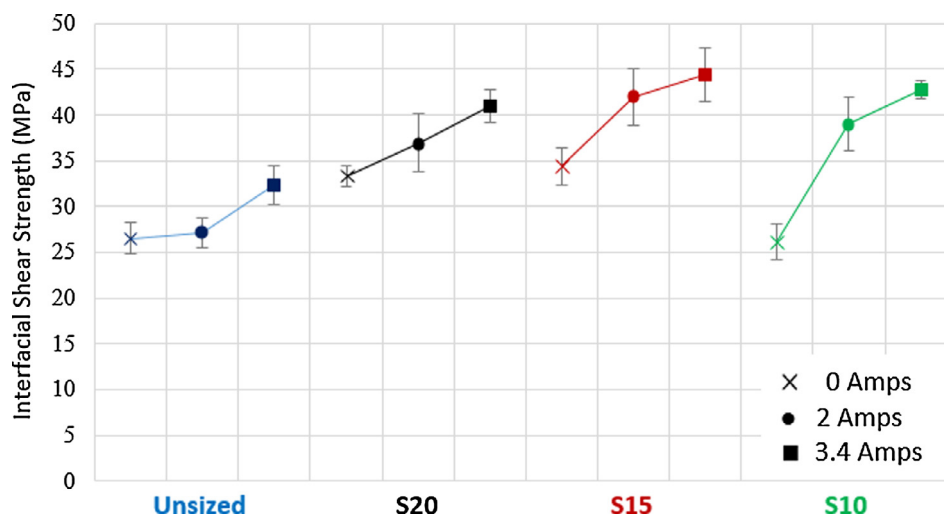
Fig. 5. Effect of amperage on IFSS in resin two. (For interpretation of the references to colour in this figure legend, the reader is referred to the web version of this article.)

Table 7
IFSS values with standard deviations for fibers in resin two.

	Unsized				S20			S15			S10	
	0 A	2 A	3.4 A	0 A	2 A	3.4 A	0 A	2 A	3.4 A	0 A	2 A	3.4 A
IFSS	27.06	26.50	32.40	33.31	36.96	40.96	34.39	41.98	44.43	27.53	38.98	42.83
SD.	1.63	1.71	2.14	1.16	4.45	1.79	1.83	0.88	2.88	2.01	2.92	0.98

Table 8
IFSS increases attributed to treatment type.

|	Fiber	Treatment	Increase[1]	Increase[2]
Control	T0-S0	NA	–	–
Δ_{SIZING}	TM-S0	2 A	+8.3 MPa	−0.56 MPa
	TH-S0	3.4 A	+11.7 MPa	+5.34 MPa
Δ_{Amps}	T0-S20	1:20 Sizing	+5.6 MPa	+6.3 MPa
	T0-S15	1:15 Sizing	+11.4 MPa	+7.3 MPa
	T0-S10	1:10 Sizing	+7.6 MPa	+0.48 MPa

[1] IFSS increases in resin one.
[2] IFSS increases in resin two.

Table 10
Pristine fibers vs desized fibers IFSS. Units MPa (Standard Dev.).

	Resin one			Resin two		
	Pristine	Desized	%*	Pristine	Desized	%*
0 A	20.4 (1.3)	21.8 (1.0)	+6.8%	25.5 (1.6)	20.8 (3.1)	−18.4%
2 A	28.7 (2.0)	30.4 (1.5)	+6.0%	26.5 (1.7)	26.7 (1.4)	+0.9%
3.4 A	32.1 (1.1)	30.5 (0.8)	−4.7%	31.7 (2.1)	26.3 (1.4)	−17.2%

* Percentage difference between pristine and desized fibers.

Table 9
Predictions vs experimental results of IFSS with deviation (Δ).

Fiber	Treatment	Predicted[1] (MPa)	Reality[1] (MPa)	Δ^1 (MPa) [%]	Prediction[2] (MPa)	Reality[2] (MPa)	Δ^2 (MPa) [%]
TM-S20	2 A, S20	34.3	31.4	(−2.9) [9.2]	33.9	36.9	(+4.2) [11.4]
TM-S15	2 A, S15	40.1	41.4	(+1.3) [3.1]	34.9	41.9	(+7.0) [19.4]
TM-S10	2 A, S10	36.3	37.8	(+1.5) [3.9]	28.5	38.9	(10.5) [30.8]
TH-S20	3.4 A, S20	37.6	32.8	(−4.6) [14.8]	38.7	40.9	(+2.3) [5.6]
TH-S15	3.4 A, S15	43.5	45.1	(+0.9) [1.9]	39.7	44.4	(+4.7) [10.6]
TH-S10	3.4 A, S10	39.6	37.8	(−1.9) [5.0]	33.3	42.8	(+9.5) [23.2]

[1] Results relating to resin one.
[2] Results relating to resin two.
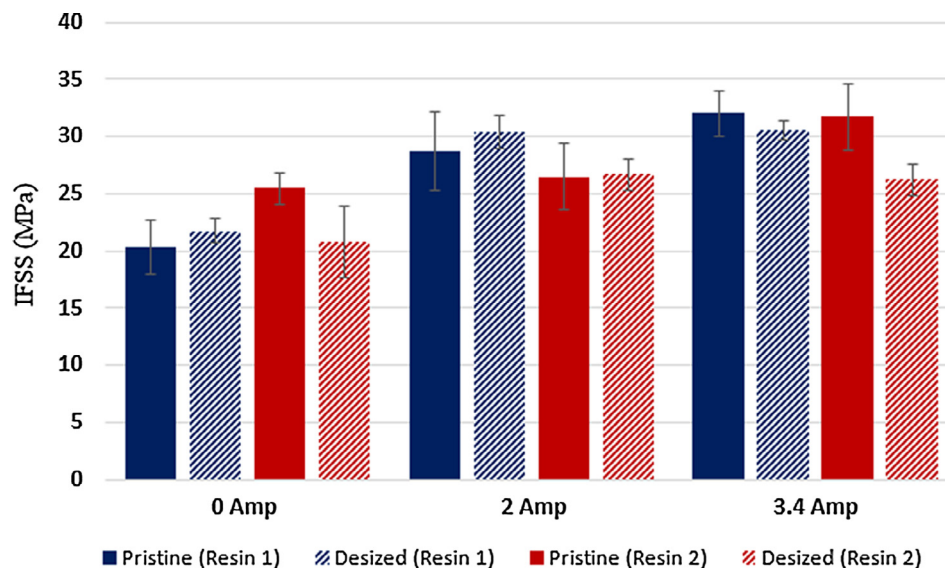
Fig. 6. Pristine fibers vs desized fibers IFSS. (For interpretation of the references to colour in this figure legend, the reader is referred to the web version of this article.)

increased amperage was also observed to decrease dispersive surface energy from between 5.8% (3.4 A, S15) to 21.5% (3.4 A, S20). This trend was not noticed in unsized fibers. Similarly the dispersive surface energies of desized and unsized fibers were observed to correlate well and be much lower than those of the sized fibers. In summary, polar surface energy remained constant regardless of treatment conditions, however dispersive energy did vary with the use of sizing (see Fig. 11).

Fig. 12 shows the relationship between IFSS and dispersive energy of all fibers in resin one. Polar energy was not mapped as variation was negligible across all fiber formats suggesting it would not influence IFSS. From Fig. 12 it is shown that no notable relationship between IFSS and dispersive surface energy exists. A linear regression analysis provides a linear coefficient of determination (r^2) value of 0.21 for resin one and 0.31 for resin two. Hence no relationship between dispersive
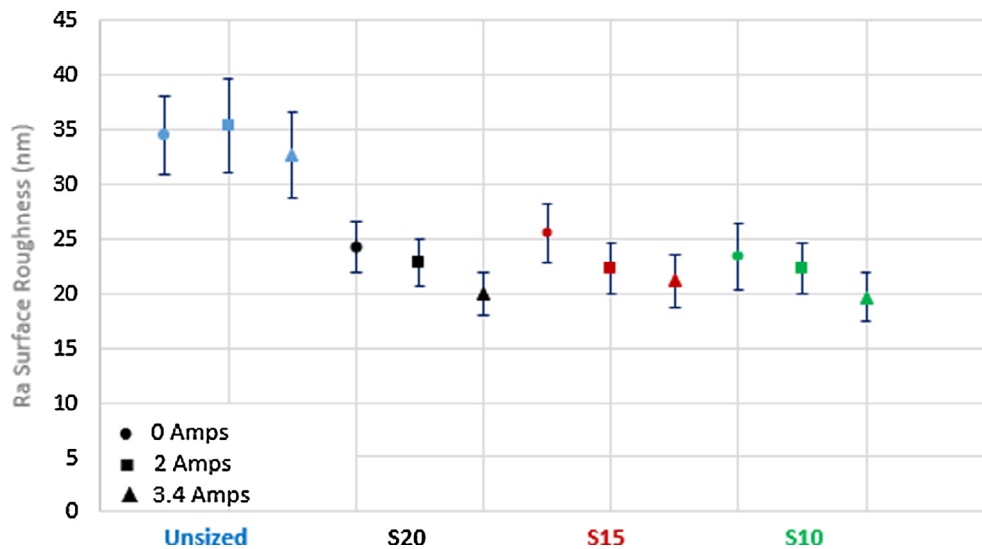
Fig. 7. Ra roughness (nm) mapped against IFSS for SFFT samples in resins one and two. (For interpretation of the references to colour in this figure legend, the reader is referred to the web version of this article.)

Table 11
Ra roughness of all fibers within study. Units nm (standard dev.).

	Unsized	Desized	S20	S15	S10
0 A	34.5 (7.2)	21.4 (4.4)	24.3 (4.6)	25.5 (5.4)	23.3 (6.1)
2 A	35.4 (8.6)	22.3 (3.5)	22.8 (4.3)	22.3 (4.6)	22.3 (4.7)
3.4 A	32.7 (7.7)	23.5 (5.2)	20.0 (3.8)	21.1 (4.8)	19.7 (4.5)

surface energy and IFSS was observed.

Importantly it must be stated that this paper is **not** suggesting that surface energy plays no role in interfacial adhesion. Rather it is important to highlight that within this study IFSS was determined using SFFT. This is a test which provides an ideal perfectly wetted microcomposite. Similarly DCAT characterisation occurred on small tow bundles that were completely saturated providing idealised results. The importance of fiber wettability in real world applications is related to the indication of resin/fiber compatibility and permeability allowing complete soaking of fibers. The results in this study simply suggest that the fibers were highly compatible however the effects of surface

chemistry on adhesion were not well suited to a IFSS comparison using SFFT.

4. Conclusion

This study showed that both sizing and oxidization amperage were able to improve IFSS. Unsized, unoxidized fibers have the lowest IFSS both epoxy resins. With the application of sizing, IFSS increased however there was an idealised ratio found at the S15 mark that provided the highest IFSS. This suggests that sizing acts as an intermediate layer at the interface that promotes adhesion however overusing or under-utilising sizing ratio in manufacturing will restrict performance potential. Electrochemical oxidization was also observed to improve IFSS with increased oxidation amperage found to increase IFSS. A 3.4 A current provided the greatest increases in IFSS however in some scenarios observed the IFSS increase between 2 A and 3.4 A was not significant suggesting that notable increases can be reached with limited oxidization. Across both resin systems the same trends were observed however trends for sizing use and oxidization were found to be more pronounced using resin one.
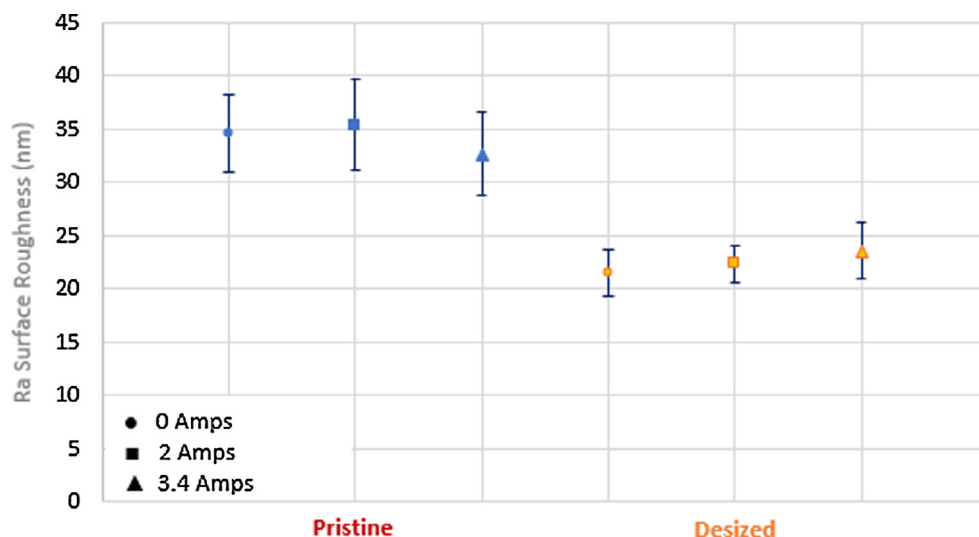

Fig. 8. Ra roughness (nm) of pristine unsized fibers versus desized fibers. (For interpretation of the references to colour in this figure legend, the reader is referred to the web version of this article.)
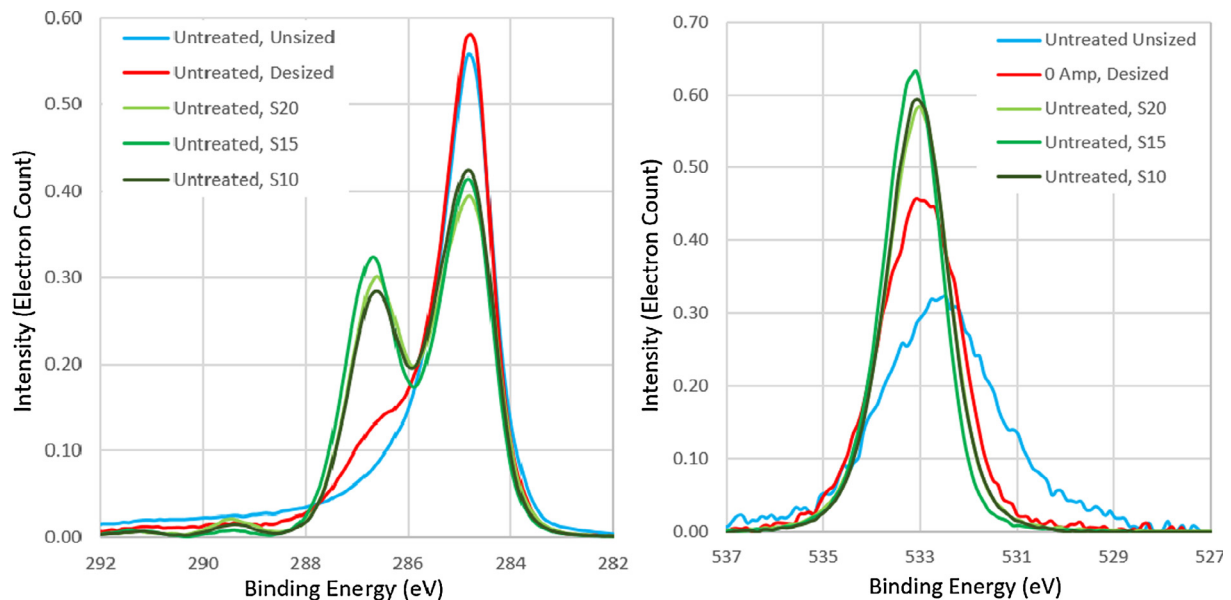
Fig. 9. XPS spectra observing sizing effects for untreated fibers. (Left) C1 spectrum. (Right) O1 spectrum. (For interpretation of the references to colour in this figure legend, the reader is referred to the web version of this article.)

Analysis of the mechanisms for improved IFSS induced by sizing and oxidization showed that each treatment improved performance independently from one another. Independent improvements by one treatment were not masked by the other. This was concluded by comparing predicted and experimentally obtained results in IFSS showing correlations within 10% for resin one.

It is concluded that oxidization amperage improved IFSS by increasing the number of oxygenated functional groups of the fiber surface thereby creating better chemical bonding at the interface, while sizing deposition improved IFSS by dispersing through the interface and acting as an intermediate junction of bonding for both the resin and fiber surface thereby facilitating adhesion. XPS results showing increased carboxylic groups with increased oxidization in all cases.

Surface roughness of fibers was observed to be greatest for unsized fibers however electrochemical oxidization did not seem to alter surface roughness to a statistically significant margin for unsized fibers. Conversely sizing was observed to decrease fiber surface roughness and

Table 12
Elemental composition values on carbon fiber surface via XPS.

Treatment	Sizing	C	N	O	Cl	Si	Na	Ca
Untreated	Unsized	1.000	0.019	0.033	0.001	0.005	0.002	0.001
2 A	Unsized	1.000	0.085	0.141	0.001	0.004	0.005	0.007
3.4 A	Unsized	1.000	0.096	0.202	0.005	0.007	0.015	0.007
Untreated	Desized	1.000	0.019	0.107	0.002	0.020	0.000	0.003
2 A	Desized	1.000	0.038	0.179	0.002	0.008	0.001	0.005
3.4 A	Desized	1.000	0.036	0.205	0.002	0.018	0.003	0.007
Untreated	S20	1.000	0.001	0.222	0.001	0.004	0.000	0.001
Untreated	S15	1.000	0.005	0.218	0.001	0.002	0.000	0.000

with increased oxidization amperage, surface roughness was decreased further. Comparatively desized fibers were seen to be significantly smoother than sized fibers. Overall surface roughness was also not observed to be the primary mechanism for increased IFSS.

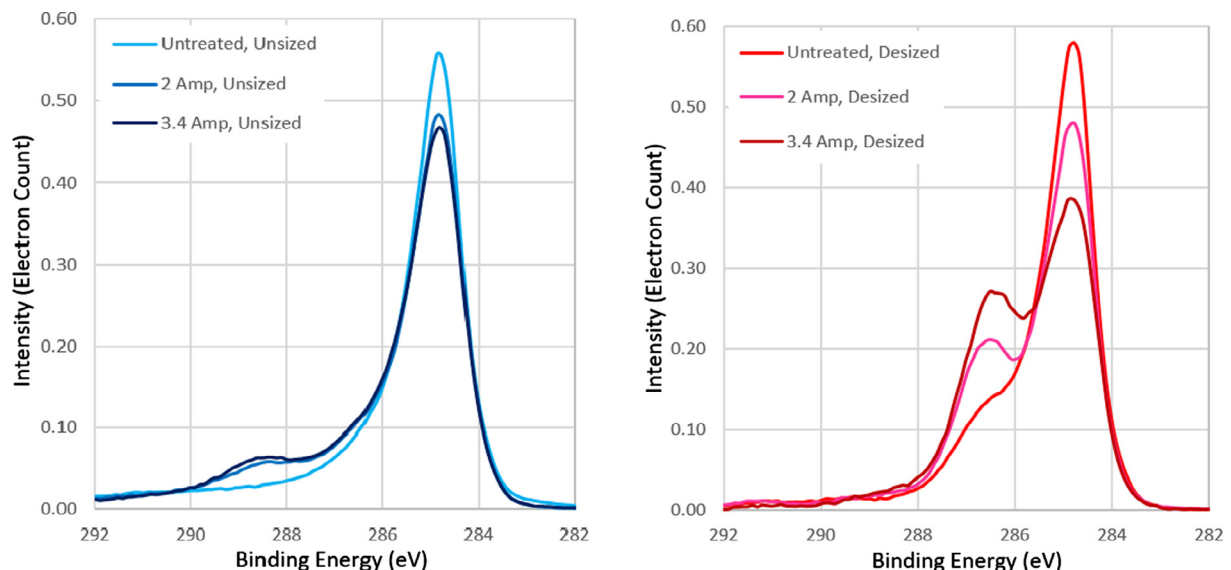Polar surface energy did not change with the addition of sizing and

Fig. 10. C1 XPS spectra. (Left) Unsized fibers with varied oxidization. (Right) Desized fibers with varied oxidization. (For interpretation of the references to colour in this figure legend, the reader is referred to the web version of this article.)

Table 13
Polar (γ_S^P) and dispersive (γ_S^D) surface energies of fibers using OWRK-(Owens-Wendt-Randal-Kaelbe method analysis.

	Polar γ_S^P (mN/m)					Dispersive γ_S^D (mN/m)				
	Unsized	Desized	S20	S15	S10	Unsized	Desized	S20	S15	S10
0 A	9.18	10.65	9.97	11.53	8.86	36.63	31.67	54.47	48.03	54.24
2 A	11.39	12.28	9.56	9.69	11.56	30.93	31.99	43.51	51.66	44.97
3.4 A	10.23	10.06	9.54	8.72	9.43	39.52	36.93	42.78	50.75	46.21
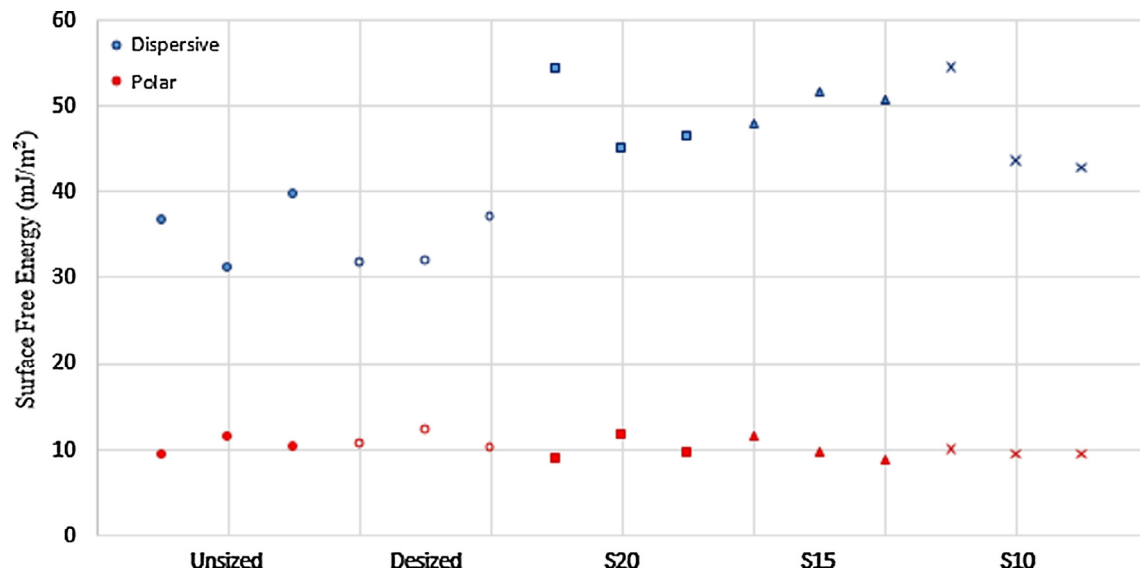
Fig. 11. Polar (γ_S^P) and dispersive (γ_S^D) surface energies of fibers using OWRK analysis. (For interpretation of the references to colour in this figure legend, the reader is referred to the web version of this article.)
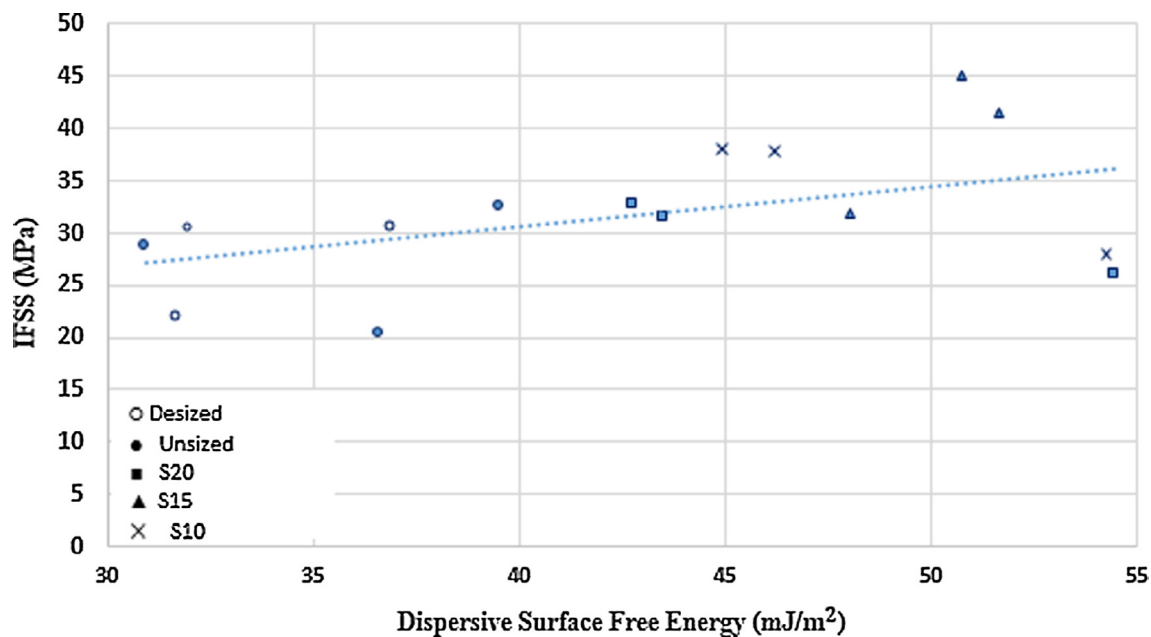

Fig. 12. Polar γ_S^P and dispersive γ_S^D surface energies compared against IFSS in RIM resin. (For interpretation of the references to colour in this figure legend, the reader is referred to the web version of this article.)

desizing. Dispersive energy was found to be significantly lower for unsized and desized fibers than those that had been sized. No correlation between surface energy and IFSS were observable.

The IFSS of pristine unsized and desized fibers showed that desized fibers done so through soxhlet extraction can be used as an accurate representative measure of pristine fiber performance however research also revealed that this may be sensitive to resin being used.

Acknowledgements

References

[1] Kamae T, Drzal LT. Carbon fiber/epoxy composite property enhancement through incorporation of carbon nanotubes at the fiber–matrix interphase – Part I: the development of carbon nanotube coated carbon fibers and the evaluation of their adhesion. Compos A 2012;43(9):1569–77.

[2] Qin W, Vautard F, Askeland P, Yu J, Drzal L. Modifying the carbon fiber-epoxy matrix interphase with silicon dioxide nanoparticles. RSC Adv 2015;5(4):2457–65.

[3] Qin W, Vautard F, Askeland P, Yu J, Drzal LT. Incorporation of silicon dioxide nanoparticles at the carbon fiber-epoxy matrix interphase and its effect on composite mechanical properties. Polym Compos 2017;38(7):1474–82.

[4] Qin W, Vautard F, Drzal LT, Yu J. Mechanical and electrical properties of carbon fiber composites with incorporation of graphene nanoplatelets at the fiber–matrix interphase. Compos B 2015;69:335–41.

[5] Downey MA, Drzal LT. Toughening of carbon fiber-reinforced epoxy polymer composites utilizing fiber surface treatment and sizing. Compos A 2016;90:687–98.

[6] Qin W, Vautard F, Drzal LT, Yu J. Modifying the carbon fiber–epoxy matrix interphase with graphite nanoplatelets. Polym Compos 2016;37(5):1549–56.

[7] Tiwari S, Bijwe J. Surface treatment of carbon fibers – a review. Procedia Technol 2014;14:505–12.

[8] Servinis L, Beggs KM, Scheffler C, Wölfel E, Randall JD, Gengenbach TR, et al. Electrochemical surface modification of carbon fibres by grafting of amine, carboxylic and lipophilic amide groups. Carbon 2017;118:393–403.

[9] Servinis L, Henderson LC, Gengenbach TR, Kafi AA, Huson MG, Fox BL. Surface functionalization of unsized carbon fiber using nitrenes derived from organic azides. Carbon 2013;54:378–88.

[10] Beggs KM, Servinis L, Gengenbach TR, Huson MG, Fox BL, Henderson LC. A systematic study of carbon fibre surface grafting via in situ diazonium generation for improved interfacial shear strength in epoxy matrix composites. Compos Sci Technol 2015;118:31–8.

[11] Raghavendran VK, Drzal LT, Askeland P. Effect of surface oxygen content and roughness on interfacial adhesion in carbon fiber–polycarbonate composites. J Adhes Sci Technol 2002;16(10):1283–306.

[12] Kaelble DH. Dispersion-polar surface tension properties of organic solids. J Adhes 1970;2(2):66–81.

[13] Dai Z, Shi F, Zhang B, Li M, Zhang Z. Effect of sizing on carbon fiber surface properties and fibers/epoxy interfacial adhesion. Appl Surf Sci 2011;257(15):6980–5.

[14] Drzal LT, Madhukar M. Fibre-matrix adhesion and its relationship to composite mechanical properties. J Mater Sci 1993;28(3):569–610.

[15] Yao L, Li M, Wu Q, Dai Z, Gu Y, Li Y, et al. Comparison of sizing effect of T700 grade carbon fiber on interfacial properties of fiber/BMI and fiber/epoxy. Appl Surf Sci 2012;263:326–33.

[16] Demir B, Henderson LC, Walsh TR. Design rules for enhanced interfacial shear response in functionalized carbon fiber epoxy composites. ACS Appl Mater Interfaces 2017;9(13):11846–57.

[17] Demir B, Beggs KM, Fox BL, Servinis L, Henderson LC, Walsh TR. A predictive model of interfacial interactions between functionalised carbon fibre surfaces cross-linked with epoxy resin. Compos Sci Technol 2018;159:127–34.

[18] Arnold CL, Beggs KM, Eyckens DJ, Stojcevski F, Servinis L, Henderson LC. Enhancing interfacial shear strength via surface grafting of carbon fibers using the Kolbe decarboxylation reaction. Compos Sci Technol 2018;159:135–41.

[19] Young III T. An essay on the cohesion of fluids. Philos Trans R Soc Lond 1805;95:65–87.

[20] Roura P, Fort J. Local thermodynamic derivation of Young's equation. J Colloid Interface Sci 2004;272(2):420–9.

[21] Jang-Kyo K, Yui-Wing M. Engineered interfaces in fiber reinforced composites. Elsevier Science Ltd; 1998.

[22] Karsli NG, Ozkan C, Aytac A, Deniz V. Effects of sizing materials on the properties of carbon fiber-reinforced polyamide 6,6 composites. Polym Compos 2013;34(10):1583–90.

[23] Feih S, Wonsyld K, Minzari D, Westermann P, Lilholt H. Testing procedure for the single fiber fragmentation test. Forskningscenter Risø 2004.

[24] Tripathi D. Single fiber fragmentation test for assessing adhesion in fiber reinforced composites. J Mater Sci 1998;33:1–16.

[25] Voleti S, Ananth C, Chandra N. Effect of interfacial properties on the fiber fragmentation process in polymer matrix composites. 1998 ASTM, CTR. 20(1). CTR10496J.

[26] Nedele MR, Wisnom MR. Three-dimensional finite element analysis of the stress concentration at a single fibre break. Compos Sci Technol 1994;51(4):517–24.

[27] Senturk Parreidt T, Schmid M, Hauser C. Validation of a novel technique and evaluation of the surface free energy of food. Foods 2017;6(4):31.

[28] Owens DK, Wendt RC. Estimation of the surface free energy of polymers. J Appl Polym Sci 1969;13(8):1741–7.

[29] Helmuth J, Schalek RL, Drzal LT. Correlation of the mechanical properties to the fiber-matrix adhesion of Nextel 312 (TM) fiber/BN/Blackglas (TM) composites. Compos Interfaces 2003;10(2–3):119–38.

[30] Oh JH, Kim JK, Lee DG, Jeong KS. Interlaminar shear behavior of thick carbon/epoxy composite materials. J Compos Mater 1999;33(22):2080–115.

[31] Beggs KM, Randall JD, Servinis L, Krajewski A, Denning R, Henderson LC. Increasing the resistivity and IFSS of unsized carbon fibre by covalent surface modification. React Funct Polym 2018;129:123–8.